Neuropathology and Applied Neurobiology (2020), **46**, 359–374 doi: 10.1111/nan.12580

An integrative correlation of myopathology, phenotype and genotype in late onset Pompe disease

M. Kulessa*, I. Weyer-Menkhoff†, L. Viergutz*, C. Kornblum‡§, K. G. Claeys¶**, I. Schneider††, U. Plöckinger‡‡, P. Young§§'§§§§, M. Boentert§§, S. Vielhaber¶¶, C. Mawrin*** , M. Bergmann†††, J. Weis‡‡‡, A. Ziagaki‡‡, W. Stenzel§§§ , M. Deschauer¶¶¶, D. Nolte****, A. Hahn††††, B. Schoser‡‡‡‡ and A. Schänzer*

**Institute of Neuropathology, Justus Liebig University, Giessen, †Institute of Clinical Pharmacology, Goethe University, Frankfurt/Main, ‡Department of Neurology, §Center for Rare Diseases, University Hospital Bonn, Bonn, Germany, ¶Department of Neurology, University Hospital Leuven, **Laboratory for Muscle Diseases and Neuropathies, Department of Neurosciences, KU Leuven, Leuven, Belgium, ††Department of Neurology, Martin Luther University Halle-Wittenberg, Halle, ‡‡Interdisciplinary Centre of Metabolism: Endocrinology, Diabetes and Metabolism, Charité-University Medicine Berlin, Berlin, §§Department of Sleep Medicine and Neuromuscular Disorders, Muenster University Hospital, Münster, ¶¶Department of Neurology, ***Institute of Neuropathology, Otto-von-Guericke University, Magdeburg, †††Institute of Clinical Neuropathology, Klinikum Bremen-Mitte, Bremen, ‡‡‡Institute of Neuropathology, RWTH University Hospital, Aachen, §§§Department of Neuropathology, Charité – Universitätsmedizin, Berlin, ¶¶¶Department of Neurology, Technical University of Munich, Munich, ****Institute of Human Genetics, ††††Department of Child Neurology, Justus Liebig University Giessen, Giessen, ‡‡‡‡Department of Neurology, Friedrich-Baur-Institute, LMU University Munich, Munich, Germany and §§§§Medical Park Reithofpark, Bad Feilnbach, Germany*

M. Kulessa, I. Weyer-Menkhoff, L. Viergutz, C. Kornblum, K. G. Claeys, I. Schneider, U. Plöckinger, P. Young, M. Boentert, S. Vielhaber, C. Mawrin, M. Bergmann, J. Weis, A. Ziagaki, W. Stenzel, M. Deschauer, D. Nolte, A. Hahn, B. Schoser and A. Schänzer (2020) *Neuropathology and Applied Neurobiology* **46**, 359–374
An integrative correlation of myopathology, phenotype and genotype in late onset Pompe disease

Aims: Pompe disease is caused by pathogenic mutations in the alpha 1,4-glucosidase (*GAA*) gene and in patients with late onset Pome disease (LOPD), genotype–phenotype correlations are unpredictable. Skeletal muscle pathology includes glycogen accumulation and altered autophagy of various degrees. A correlation of the muscle morphology with clinical features and the genetic background in *GAA* may contribute to the understanding of the phenotypic variability. **Methods**: Muscle biopsies taken before enzyme replacement therapy were analysed from 53 patients with LOPD. On resin sections, glycogen accumulation, fibrosis, autophagic vacuoles and the degree of muscle damage (morphology-score) were analysed and the results were compared with clinical findings. Additional autophagy markers microtubule-associated protein 1A/1B-light chain 3, p62 and Bcl2-associated athanogene 3 were analysed on cryosections from 22 LOPD biopsies. **Results**: The myopathology showed a high variability with, in most patients, a moderate glycogen accumulation and a low morphology-score. High morphology-scores were associated with increased fibrosis and autophagy highlighting the role of autophagy in severe stages of skeletal muscle damage. The morphology-score did not correlate with the patient's age at biopsy, disease duration, nor with the residual GAA enzyme activity or creatine-kinase levels. In 37 patients with LOPD, genetic analysis identified the most frequent mutation, c.-32-13T>G, in 95%, most commonly in combination with c.525delT (19%). No significant correlation was found between the different *GAA* genotypes and muscle morphology type. **Conclusions**:

Correspondence: Anne Schänzer, Institute of Neuropathology, Arndstr.16, 35392 Giessen, Germany. Tel: 0049 641-9941184; Fax: 0049 99641-41189; E-mail: anne.schaenzer@-patho.med.uni-giessen.de

Muscle morphology in LOPD patients shows a high variability with, in most cases, moderate pathology. Increased pathology is associated with more fibrosis and autophagy.

Keywords: autophagy, GAA, genotype, GSD II, late onset Pompe disease (LOPD), lysosomal storage disease

Introduction

Pompe disease (OMIM 232300) is an autosomal recessive disease caused by a defect in the lysosomal alpha glucosidase due to bi-allelic pathogenic mutations in the alpha 1,4-glucosidase gene (*GAA*). *GAA* is located on chromosome 17q25.2–25.3 and contains 20 exons resulting in a protein of 952 amino acids [1]. Nowadays, more than 500 variants of mutations in *GAA* are known, which are listed at the Pompe Disease Mutation Databank (http://www.pompevariantdatabase.nl/) and are associated with a severity ranking by determining GAA enzyme activity [2–4]. However, the clinical phenotypes associated with most of the pathogenic variants show a high variability without clear genotype-phenotype correlation, which makes prediction of the disease outcome difficult [2–9].

Infants with infantile onset Pompe disease (IOPD) are associated with pathogenic variants, e.g. c.525delT, c.2481+102_2646+13del, that affect both alleles severely, resulting in near absence of GAA enzyme activity (<1%), an age of onset below 12 months, hypertrophic cardiomyopathy and poor outcome, at least in the patients not treated with enzyme replacement therapy (ERT) in time [10–14].

In individuals with late onset Pome disease (LOPD), the pathogenic variant c.32-13T>G is the most common and is associated with a milder phenotype [9,11,12,15]. In German LOPD patients, the c.-32-13T>G mutation is also the most common. The missense mutations c.307T>G and c.877G>A are more common in German patients than in the other European patients [16–18]. In individuals with LOPD, treatment with ERT reduces muscle weakness, respiratory insufficiency and mortality [19,20]. The GAA enzyme defect leads to lysosomal and extra-lysosomal accumulation of glycogen in striated muscles with disorganization of myofibrillar architecture and loss of function of the muscle cell [17,21–23]. In addition, disturbed autophagy contributes to the muscle pathology and autophagic vacuoles (AV) are frequently present in muscle biopsies from patients with Pompe disease [21,24–29]. ERT leads to glycogen clearance in skeletal muscle from the individuals with IOPD and LOPD. Nevertheless, severely abnormal microscopic findings in skeletal muscle at the start of therapy are associated with a worse clinical outcome [21,22,29,30]. Also, muscle pathology can progress even on ERT, a phenomenon, which is not well understood. The aim of the present study was to analyse the muscle morphology of 53 patients with LOPD in detail and compare these findings with the clinical data. Histopathological changes were correlated with individual genotypes in 37 patients. To our knowledge, this is the largest cohort of detailed muscle biopsy analysis in LOPD, and individual correlation of detailed muscle morphology with the *GAA* genotype has not been described before.

Materials and methods

Patients

Patients with LOPD who underwent a muscle biopsy were included in this study. In all 53 patients, a muscle biopsy was taken for diagnostic purposes before ERT was started. Muscle biopsy location was chosen based on the clinical presentation of the myopathy (Table S1). The diagnosis of Pompe disease was confirmed by a reduction in GAA enzyme activity and/or genetic testing. We included all available muscle biopsy tissue samples from confirmed Pompe patients though the German Neuromuscular centre network. The patients have been seen and examined at different Pompe centres in Germany and resin embedded muscle tissue and cryosections were provided from the associated laboratories. Clinical data were collected retrospectively. Data on enzyme activity levels were available in 26 patients with samples derived from either dried blood spot or muscle tissue. The GAA enzyme activity levels were stated as the percentage of normal values. The *GAA* mutations were available for 37 patients and expected effects were categorized according to the

Pompe Disease Mutation Database as potentially mild, severe or unknown phenotype (Table 1) [4]. Clinical data on the duration of symptoms prior to biopsy were available in 30 patients. Serum creatine kinase (CK) at the time of biopsy was available in 39 patients (Table S1).

Muscle pathology analysis

Resin sections and transmission electron microscopy Small samples were taken from open muscle biopsies and fixed in 4% glutaraldehyde/0.4MPBS and processed according to standard procedures. One to two μm semithin sections were cut from resin embedded tissue and stained with Periodic acid-Schiff (PAS) and 2%-p-phenyldiamine (PPD) [21]. Morphometric analysis of glycogen accumulation, large empty vacuoles (LEV) and pathology score were performed on PAS-stained resin sections using a light microscope equipped with a motorized stage and digital camera with newCAST software as described before [21]. In brief, the section was delineated and a point grid containing 256 crosses was projected to each field of view. For estimating glycogen deposits and LEV, the area below the points were graded as PAS positive, PAS negative or LEV and estimated as percentage of total area [%/muscle fibre (MF)]. For estimating the muscle score, area below the points were graded from 0 to 5 according to the previously described criteria (grade 0 = normal, grade 1 = small PAS + vacuoles, grade 2 = medium PAS + vacuoles, grade 3 = larger PAS + vacuoles with myofibrillar disruption, grade 4 = larger PAS + vacuoles and LEV with myofibrillar disruption, grade 5 = LEV with myofibrillar disruption) (Figure S1A–C). A morpho-score was calculated (x% grade0 × 0) + (x%grade1 × 1) + (x% grade2 × 2) + (x%grade3 × 3) + (x% grade4 × 4) + (x%grade5 × 5)/100 from these findings expressed in grade 1–5 with 0 as lowest grade demonstrating normal morphology [21].

Muscle fibres with AV (vacuoles with dark inclusions) were analysed on PPD stained resin sections as percentage of all MFs. Additionally, the degree of fibrosis was estimated semi-quantitatively on PAS stained resin sections and rated from normal (0) to severe (3) (Table S2). For contrast in transmission electron microscopy (TEM), ultrathin sections were treated with 3% lead citrate-$3H_20$ with a Leica EM AC20 (ultrastain kit II, Leica Microsystems, Wetzlar, Germany) and examined at a Zeiss EM109 TEM (Carl Zeiss Microscopy GmbH, Jena, Germany) equipped with a sharp eye digital camera.

Histochemical, immunohistochemical and immunofluorescence microscopy In a smaller cohort (n = 22), unfixed muscle tissue was available for additional enzymatic and immunohistological staining for autophagy and lysosomal markers. Unfixed tissue was snap frozen and 6 μm cryosections were stained for the lysosomal enzyme, acid phosphatase according to

Table 1. Mutations in *GAA* in 37 patients were matched and ranked according to the Pompe Disease Mutation Database (http://www.pompevariantdatabase.nl/)

Patient	*Allele 1*	*Allele 2*
P3	c.-32-13T>G	c.525delT
P17	c.-32-13T>G	c.525delT
P24	c.-32-13T>G	c.525delT
P30	c.-32-13T>G	c.525delT
P58	c.-32-13T>G	c.525delT
P51	c.-32-13T>G	c.525delT
P52	c.-32-13T>G	c.525delT
P9	c.-32-13T>G	c.794delG
P10	c.-32-13T>G	c.794delG
P1	c.-32-13T>G	c.1076-1G>A
P8	c.-32-13T>G	c.1548G>A
P13	c.-32-13T>G	c.2078_2079insA
P25	c.-32-13T>G	c.2608C>T
P28	c.-32-13T>G	c.1822
P34	c.-32-13T>G	c.118C>T
P37	c.-32-13T>G	c.2242G>T
P41	c.-32-13T>G	c.271delG
P42	c.-32-13T>G	c.118C>T
P11	c.-32-13T>G	c.1495T>A
P12	c.-32-13T>G	c.307T>G
P15	c.-32-13T>G	c.1655T>C
P16	c.-32-13T>G	c.925G>A
P18	c.-32-13T>G	c.1942G>A
P19	c.-32-13T>G	c.2055C>A
P20	c.-32-13T>G	c.1829C>T
P21	c.-32-13T>G	c.1064T>C
P22	c.-32-13T>G	c.1075 G>A
P32	c.-32-13T>G	c.1655T>C
P36	c.-32-13T>G	c.655G>A
P4	c.-32-13T>G	c.2407C>T
P6	c.-32-13T>G	bp del (IVS16+102_IVS17+31)
P29	c.-32-13T>G	c.1127delGGinsC
P23	c.-32-13T>G	/
P27	c.-32-13T>G	/
P14	c.1655T>C	c.1478C>T
P40	c.1478C>T	/
P53	536bpdel	c.-32-13T>G

Red = severe; blue = mild; grey = unknown clinical phenotype.

standard procedures [31]. Immunohistochemical analysis was performed on cryosections using a Bench Mark XT automatic staining platform (Ventana, Heidelberg, Germany) with the following primary antibodies: mouse monoclonal anti-microtubule-associated protein 1A/1B-light chain 3 (LC3) (0231-100/LC3-5F10, nanoTools, 1:100, Teningen, Germany); mouse monoclonal anti-p62 (610832, BD Biosciences, 1:500, Franklin Lakes, NJ, USA). The following primary antibodies were used for immunofluorescence: mouse monoclonal anti-desmin (M076029-2, Agilent, 1:100, Santa Clara, CA, USA); rabbit polyclonal anti-Bcl2-associated athanogene 3 (BAG3) (10599-1-AP, Proteintech, 1:500, Manchester, UK). The secondary antibodies were: Alexa Fluor 568 goat anti-rabbit IgG (Life Technologies, 1:100, Carlsbad, CA, USA) and Alexa Flour 488 goat anti-mouse (Life Technologies, 1:500). The sections were mounted with Fluoroshield mounting medium with DAPI (Abcam, Cambridge, UK) and examined using a Nikon Eclipse 80i or Leica DM2000 fluorescence microscopes. The intensity of acid phosphatase staining was estimated semi-quantitatively and rated from normal or absent (0) to strong (4), LC3 and p62 was estimated semi-quantitatively and rated from normal or absent (0) to strong (3). Muscle sections stained with antibodies against desmin and BAG3 were estimated for BAG3 positive inclusions and rated from absent (0) to strong (3).

Statistics Correlations between the morphological score and clinical data and autophagy markers were analysed by calculating the Spearman rank correlation coefficient to asses a possible linear association between two variables. To analyse differences between the genetic combination with regard to score, age and GAA enzyme activity Kruskal–Wallis-test was used. Data were analysed using the R software package (version 3.4.3 for Windows; https://CRAN.R-project.org, R Core Team, [51]).

Results

Patients

Muscle biopsy specimens from 29 (55%) male, age at biopsy varying between 16–78 years (median 46 year), and 24 (45%) female patients, age at biopsy between 14–72 year (median 42 year), were analysed. The distribution of gender and age in this study was similar to those in other studies [29]. Patients were 14−78 years of age (n = 53, median 44 year) at time of biopsy, with n = 29 (55%) between 30 and 50 years. Disease onset was at 8–73 years (n = 33; median 39 year) with a diagnostic delay to the time of biopsy and disease duration of 0–26 years (n = 33, median 5 year) (Figure 1**A** and Table S1).

Muscle pathology

Morpho-score The analysis of the muscle biopsies (n = 53) showed high variability in the morpho-score [0.59 (0.07–3.77)], glycogen accumulation [4.73 (0.24–44.62) PAS+ %/MF], LEV [0.06 (0–10.09) LEV%/MF] and AV [n = 48, 2.68 (0–27.56) AV%/MF]. Forty patients (75%) showed <10% PAS/MF glycogen accumulation and 68% (36/53) a low morpho-score (<1) (Figure 1**B** and Table S2).

The morpho-score significantly correlated with fibrosis (Spearman's $\rho = 0.46$; $P = 0.0006$) showing remodelling of connective tissue in severe stages. The analysis of AV showed a significant positive correlation with the morpho-score (Spearman's $\rho = 0.34$; $P = 0.0173$), highlighting the role of autophagy during muscle pathology progression. The morpho-score significantly correlated with glycogen accumulation (PAS) (Spearman's $\rho = 0.86$; $P < 0.0001$) and LEV (Spearman's $\rho = 0.35$; $P = 0.01$) as was to be expected since both parameters are included in the morpho-score (Figure 2).

TEM Samples with different degrees of pathology were examined at the ultrastructural level. Muscle biopsies with a low morpho-score mainly showed lysosomal glycogen and normal sarcomeric architecture (Figure 3**A**,**C**,**E**). Biopsies with high morpho-scores showed massive lysosomal and non-lysosomal glycogen deposits with sarcomere disorganization (Figure 3**B**,**D**, **F**). Additionally, AV were more prominent in biopsies with high morpho–scores, often accompanied by abnormal mitochondria with increased variation of size and disruption of cristae structure (Figure 4**A**–**F**). In many biopsies with low morpho-scores, in addition to lysosomal glycogen, intermyofibrillar glycogen was present (Figure 5**A**,**B**). In biopsies with higher scores, extra-lysosomal glycogen surrounding lysosomes was

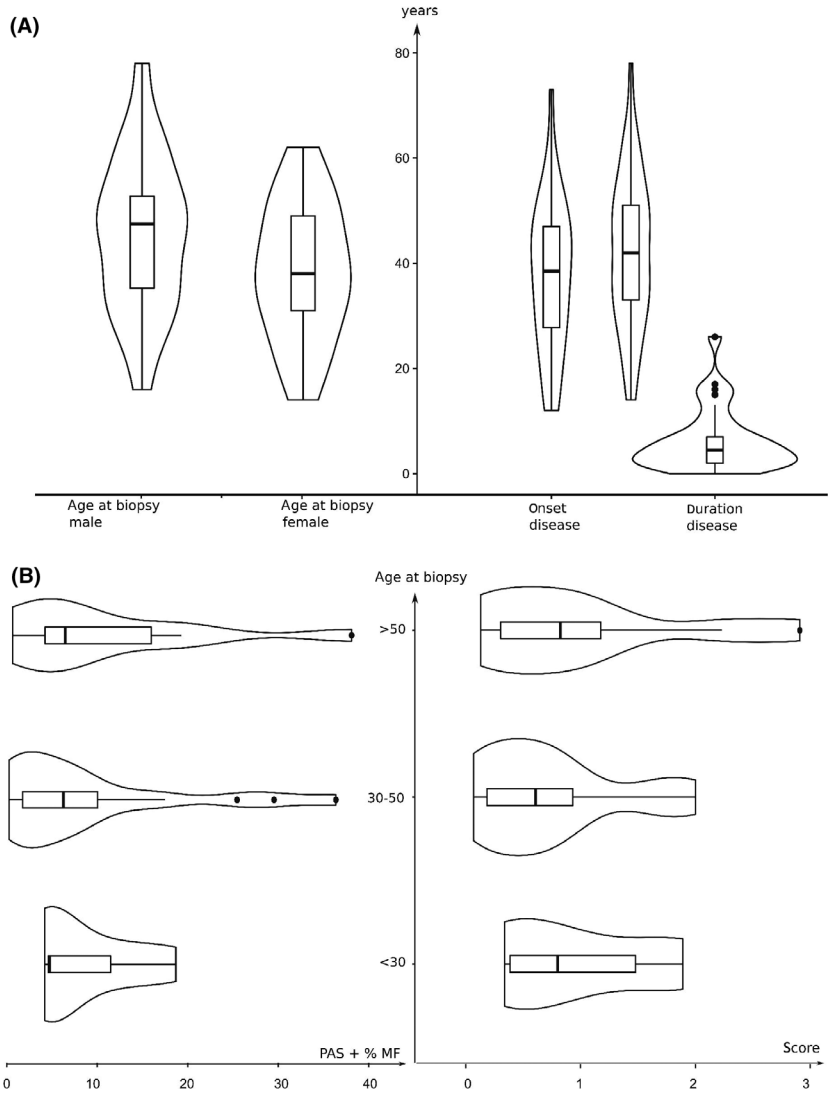

Figure 1. Analyses of clinical data compared to muscle morphology. Patients analysed are equally distributed in gender (male 55%) with no difference at age at biopsy. The age at symptom onset varies from 8 to 73 years (median 39 year) and age at biopsy from 14 to 78 years (median 44 year) with a duration of symptoms before biopsy of 0–26 years (median 5 year) (**A**). The majority of patients are between 30–50 years old and have glycogen accumulation < 10 PAS%/muscle fibre (MF) (75%) and a low morpho-score < 1 (68%) without differences in muscle morphology between different age groups (**B**). The superimposed box and whisker plots have been constructed using the quartiles and medians (solid horizontal line within the boxes). The lines add 1.5 times the interquartile range (IQR) to the 75th percentile or subtract 1.5 times the IQR from the 25th percentile and are expected to include 99.3% of the data. They are surrounded by violin plots showing the density distribution of the values.

often seen in combination with autophagosomes with double layered membranes and autophagic material (Figure 5**C**,**D**).

Enzymatic staining for acid phosphatase and expression of antibodies against autophagy markers p62, LC3 and BAG3 Staining intensity of acid phosphatase and expression of autophagy markers LC3 and p62 in 22 muscle biopsies showed a stronger upregulation in muscle biopsies graded with a higher morpho-score and increased AV. The analysis of the morpho-score showed a significant positive correlation with p62 (Spearman's $\rho = 0.48$; $P = 0.031$) and acid phosphatase (Spearman's $\rho = 0.70$; $P = 0.0006$) compatible with increased autophagy during Pompe disease progression (Figure S2**A**,**B** and Table S3).

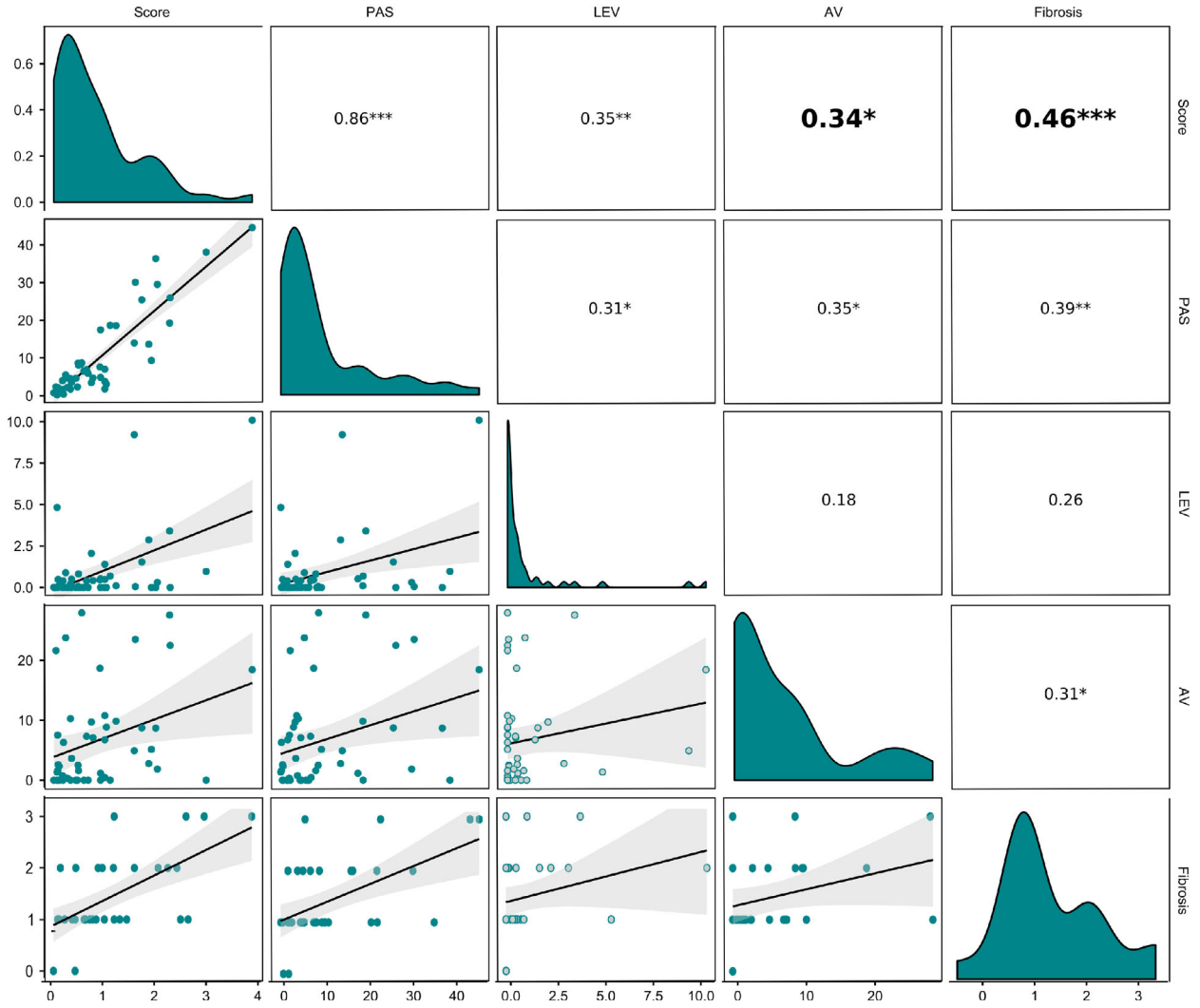

Figure 2. Correlation matrix of morpho-score, glycogen accumulation, large empty vacuoles (LEV), autophagic vacuoles (AV) and fibrosis obtained from the muscle biopsies. For estimating the muscle pathology PAS and 2%-p-phenyldiamine stained resin sections were analysed by a recently established morpho-score. Upper triangular part of the matrix shows the Spearman correlation coefficients (Spearman's rho with significance levels associated to a symbol (*P*-values: ***<0.001, **<0.01, *<0.05) or conditional (split according to levels) boxplots. The distribution of each variable is shown on the diagonal (green). Lower triangular part of the matrix shows the bivariate scatterplots (green) with a fitted line (black) and the confidence interval of the line (grey) or histograms were separated according to levels. The morpho-score significantly correlates with fibrosis and AV showing remodelling of connective tissue and increased autophagy during muscle pathology progression (bold).

Double immunofluorescent staining against Z-band proteins desmin and BAG3 was performed at 22 biopsies. In the majority of biopsies, small BAG3 positive aggregates were present mainly in the core of well-preserved fibres and were increased in biopsies of high p62 and LC3 expression. In comparison, in MFs with large vacuoles (LEV), there was co-expression of desmin and BAG3 in the peripheral area reflecting remnants of Z-band structures and no BAG3 positive inclusions were detected. At TEM, large autophagosomes were mainly seen in the core of MFs with normal sarcomere structures whereas they were not present in MFs with abundant LEV (Figure S4). These findings suggest that BAG3 plays a role in early, but not late stage in the single MF pathology. Interestingly, one patient (P28) with a high number of AV showed high expression of LC3, p62 and BAG3 consistent with increased autophagy even at a moderate score (0.38) and glycogen

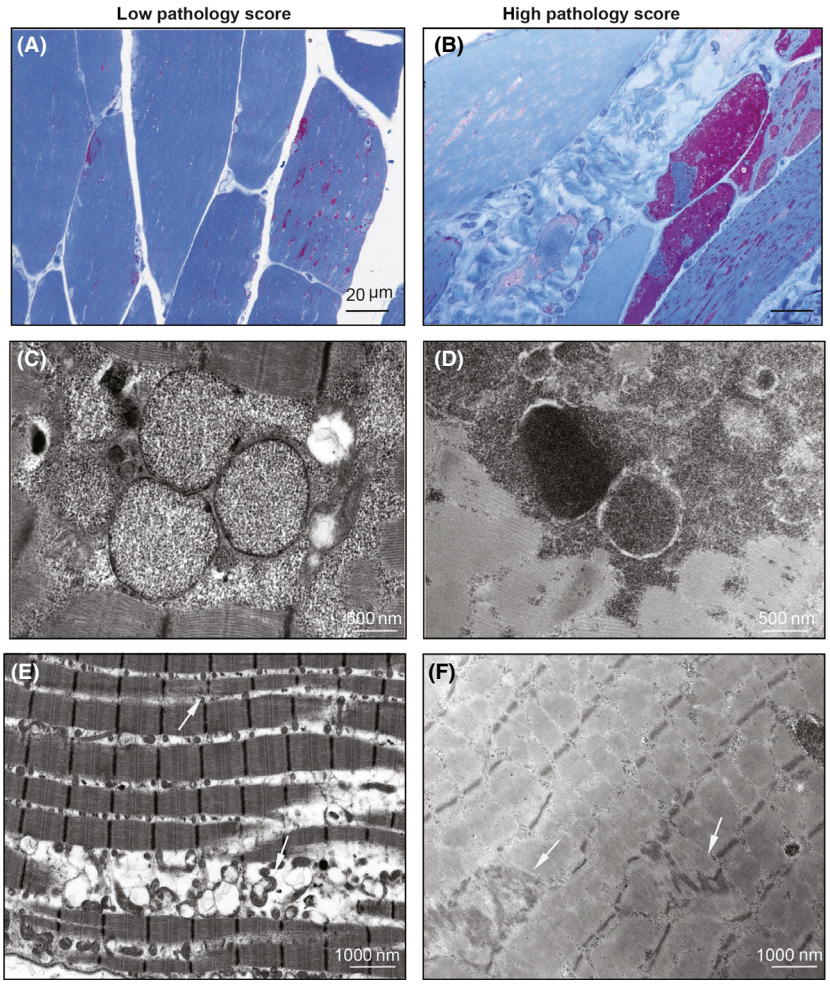

Figure 3. Muscle biopsy specimens from two patients with different grade of muscle pathology. P16 demonstrates a low morpho-score of 1.02 with moderate increased spectrum of muscle fibre (MF) diameters without endomysial fibrosis (PAS%/MF = 7.04, LEV = 0.48 and AV = 0.45) (**A**). On ultrastructural analysis, P16 shows lysosomal glycogen and small extra-lysosomal glycogen deposits (**C**). The sarcomere architecture is mostly well organized with only a few dispersed Z-bands and marginal mitochondrial pathology with aggregation and deranged cristae (**E**). P30 shows a high morpho-score of 2.23 with increased MF size variation and pronounced endomysial fibrosis (PAS%/MF = 19.29, LEV%/MF = 3.41 and AV%/MF = 27.56) (**D**). On ultrastructural analysis, P30 shows lysosomal and extra-lysosomal glycogen (**D**) with disorganization of the sarcomeric structures with Z-band streaming (**F**) (**A**,**B**: PAS stained resin sections). (PAS, Periodic acid-Schiff; LEV, large empty vacuoles; AV, autophagic vacuoles).

accumulation (4.19%). The biopsy was taken at 14 years of age (the youngest patient in the study) with the *GAA* mutations c.-32-13T>G, c.1822C>T (Figure S3 and Table S3).

Muscle pathology and clinical findings The morpho-score showed no significant correlation with the age at biopsy, disease duration (years from first symptoms to biopsy) and GAA enzyme activity ($n = 26$), 18% (3.8–39%) ($P > 0.3$) and CK levels [$n = 39$, median 536, (96–1767 U/I)] CK levels showed a significant negative correlation with the age at biopsy (Spearman's $\rho = -0.54$; $P = 0.0004$) (Figure 6).

Genotype, clinical phenotype and muscle morphology type In 37 patients, 26 known pathogenic mutations in *GAA* were detected. Among those, the majority (95%) were the common splice site mutation c.-32-13T> G, followed by the deletion mutation c.525delT (19%). Other mutations were c.1655T>C (8%), c.1478C>T (5%), c.118C>T (5%) and c.794delG (5%). The most common combination ($n = 7$, 19%) was c.-

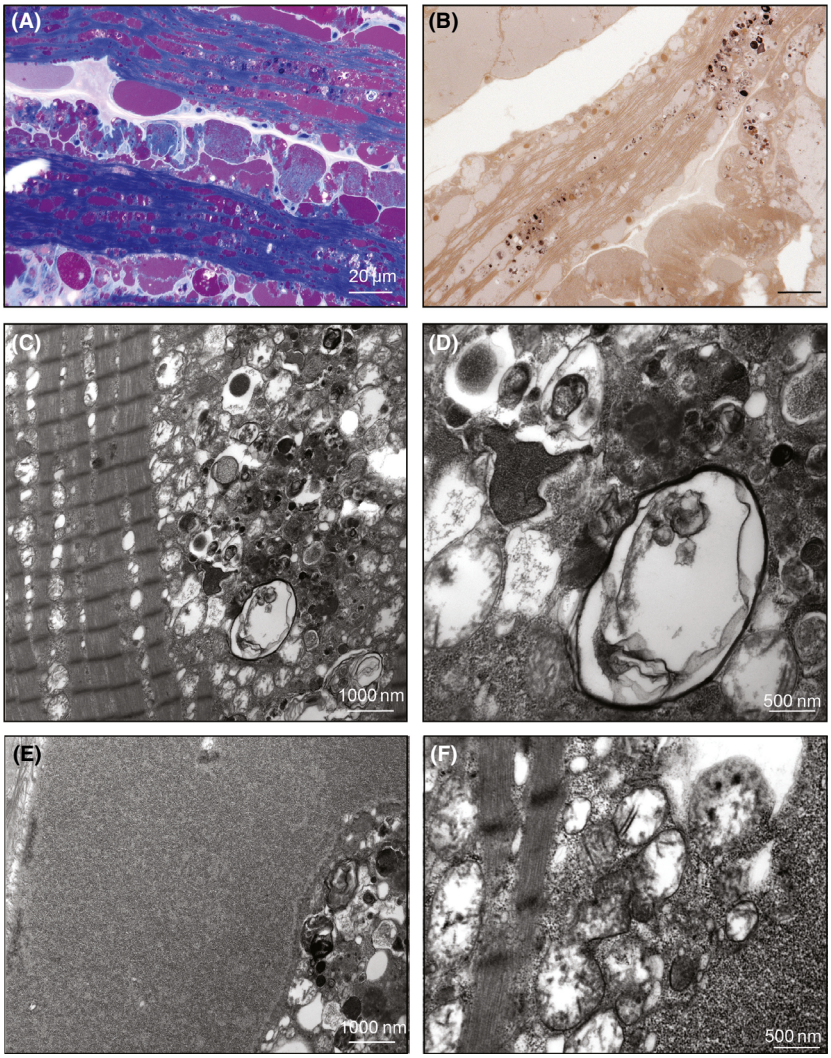

Figure 4. Estimation of glycogen accumulation and AV in muscle biopsy specimens from a patient with a high morpho-score. Disturbed autophagy is a hallmark of Pompe disease and AV increase with the morpho-score and glycogen accumulation. On resin sections, autophagy can be estimated by the amount of the AV and LEV. Patient (P2) with a high morpho-score of 3.77 with an abundant glycogen accumulation (PAS%/MF = 44.6%), vacuoles (AV = 18.43, LEV = 10.09), and endomysial fibrosis (grade 2): pronounced muscle pathology and massive glycogen accumulation in PAS-stained sections (**A**) with prominent AV detectable in PPD stained sections with dark inclusions (**B**). Transmission electron microscopy shows AV containing myelin-like structured debris (**C**,**D**), and are located adjacent to the sarcomeres or massive glycogen deposits (**C**,**E**). Mitochondria are focally accumulated and swollen with disrupted internal cristae structures (**F**). (PAS, Periodic acid-Schiff; LEV, large empty vacuoles; AV, autophagic vacuoles; PPD, p-phenyldiamine).

32-13T>G together with c.525delT. In three patients (8%), only a single mutation on one allele was identified (Figure 7 and Table 1).

We were interested in comparing genotype data to the clinical phenotype and muscle morphology data. Therefore, the mutations in *GAA* were ranked according to the Pompe Disease Mutation Database (http://www.pompevariantdatabase.nl/) as 'severe' (very severe mutation), 'mild' (potentially less severe mutation) or 'unknown' phenotype [2–4]. Applying this ranking clustered the patients into six different groups (score and age shown as medians): patients with two mutations predicted to be 'mild' [n = 11, score: 0.53 (0.07–2.9), n = 9 age of onset: 43 year (15-73 year)], patients with one mutation predicted to be 'mild' and one to be 'severe' [n = 18, score 0.70, 0.14–2.23, n = 15, age of onset, 36 (13–55 year)], patients with one mutation predicted to be 'mild' and one 'unknown'

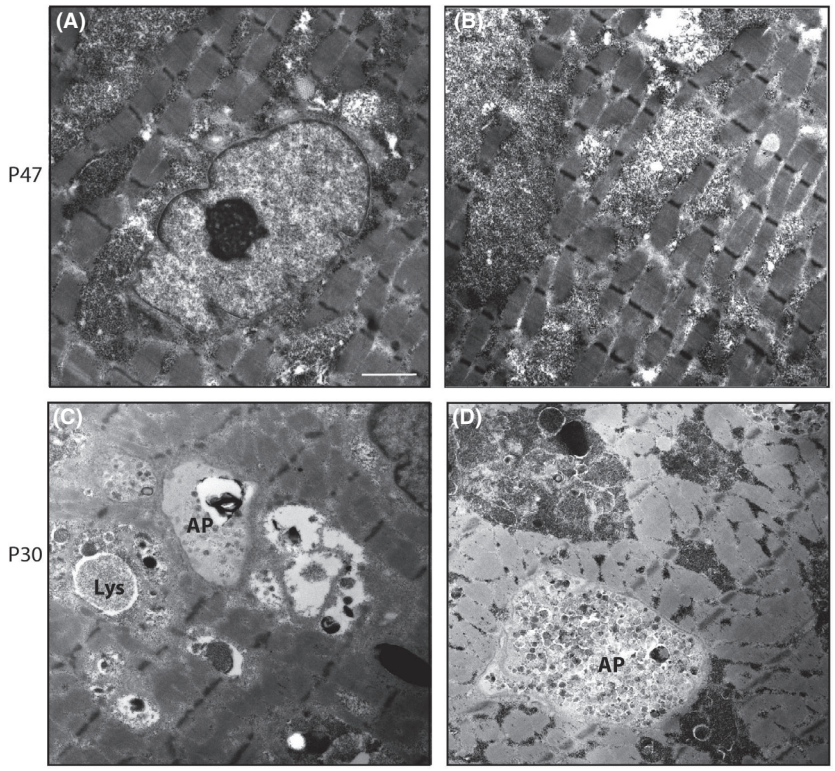

Figure 5. Lysosomal and extra-lysosomal glycogen deposits and autophagosomes at transmission electron microscopy. Muscle biopsy P47 with a moderate score = 1.59 and glycogen accumulation of PAS%/MF = 30.1% shows frequent extra-lysosomal glycogen with no severe disturbance of sarcomeric structures (**A**,**B**). Muscle biopsy from P30 with a high score = 2.23 with frequent enlarged glycogen containing lysosomes, extra-lysosomal glycogen and large autophagosomes (**C**,**D**) (Lys, lysosome; AP, autophagosome).

[n = 3, score 0.37 (0.13–1.57), n = 3, age of onset: 43 year (27–58 year)] and patients with one mutation predicted to be 'mild' only [n = 2, score 1.39 (0.94–1.84), age of onset 22 year (12–32 year)], patient with one 'unknown' and one predicted to be 'mild' (n = 1, score 0.71, age of onset 55 year) and 'unknown' mutation at one allele (n = 1, score 0.87, age at onset 49 year) (Table 1 and Figure 7). The ranked means of the allele combinations for morpho-score, disease onset and GAA enzyme levels were equally distributed as the p-values did not meet statistical significance ($P > 0.4$). In particular, the ranked means of the most common combination of mutation c.-32-13T>G; c.525delT [n = 7, score 0.94, 0.14–2.23; age of onset: 45 year, (20–55 year)] for score, disease onset and GAA enzyme levels were equally distributed compared to mutation combination c.-32-13T>G and other [n = 28, score: 0.59 (0.07–2.9), n = 22, age of onset: 39 year (13–73 year)] and combination non c.-32-13T>G and other [n = 3, score 0.87 (0.71–1.57), n = 2, age of onset: 33.5 year (27–40 year)] (Figure 7).

Additionally, no significant differences were detectable analysing the vacuoles (AV or LEV) with respect to the *GAA* genotype (Figure S5).

Discussion

Investigation of muscle biopsies gives a great opportunity to analyse disease pathogenesis and may add to the understanding of the broad clinical variability in LOPD. The aim of our study was a detailed analysis of muscle morphology from a large cohort of patients with LOPD before the start of ERT and comparison of these findings to the clinical, laboratory (GAA enzyme activity, CK levels) and pathogenic variants in *GAA*.

For grading the muscle pathology, we used a morpho-score, which we had already established on resin embedded biopsies from patients with IOPD [21]. The morpho-score includes, in addition to glycogen accumulation, myofibrillar disruption and LEV as a feature of disturbed autophagy. In IOPD patients, a lower score reflecting less pathology is associated with a better

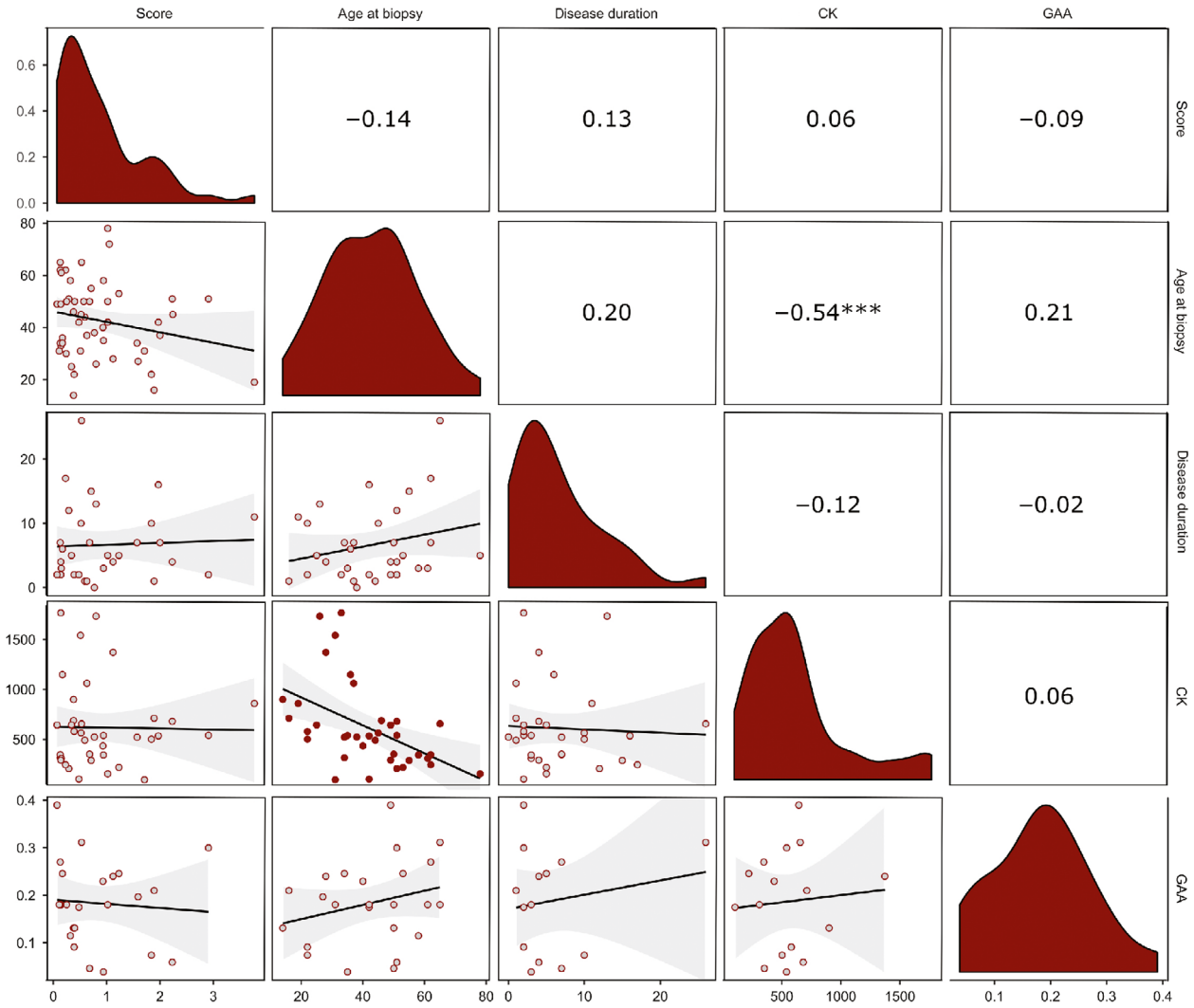

Figure 6. Correlation matrix of morpho-score, age at biopsy, disease duration, creatine kinase (CK) and alpha 1,4-glucosidase (GAA) residual enzyme activity obtained from the patients. Upper triangular of the matrix shows the Spearman correlation coefficients (Spearman's ρ) with significance levels associated to a symbol (*P*-values: ***<0.001, **<0.01, *<0.05). The distribution of each variable is shown on the diagonal (red). Lower triangular part of the matrix shows the bivariate scatterplots (red) with a fitted line (black) and the confidence interval of the line (grey). The morpho-score shows no significant correlation with clinical symptoms and GAA residual enzyme activity, CK levels are significantly negative correlated with the age at biopsy.

response to ERT with recombinant GAA, whereas patients with a high morpho-score have a limited ERT response [21]. The data are in line with other reports showing a worse response to therapy in patients with severely damaged MFs with worse pathology indicating the need for early therapy in patients with minor

Figure 7. Analyses of alpha 1,4-glucosidase (*GAA*) mutations compared to muscle morphology and clinical data. Boxplots of the individual morpho-score to *GAA* mutation combination. The combinations for each subject are shown as points, and the box and whisker plots show the quartiles and medians (solid horizontal line within the boxes). The whiskers add 1.5 times the interquartile range (IQR) to the 75th percentile or subtract 1.5 times the IQR from the 25th percentile. According to the Pompe Disease Mutation Database, mutations were ranked as mild (potential less severe mutation); severe, (very severe mutation); unknown, (unknown mutation) and no single nucleotide polymorphism (SNP). The global differences between the individual scores to mutation combination did not meet statistical significance ($P > 0.1$). The ranked means of the *GAA* allele combinations for (A) morpho-score, (B) disease onset and (C) GAA residual enzyme activity are equally distributed.

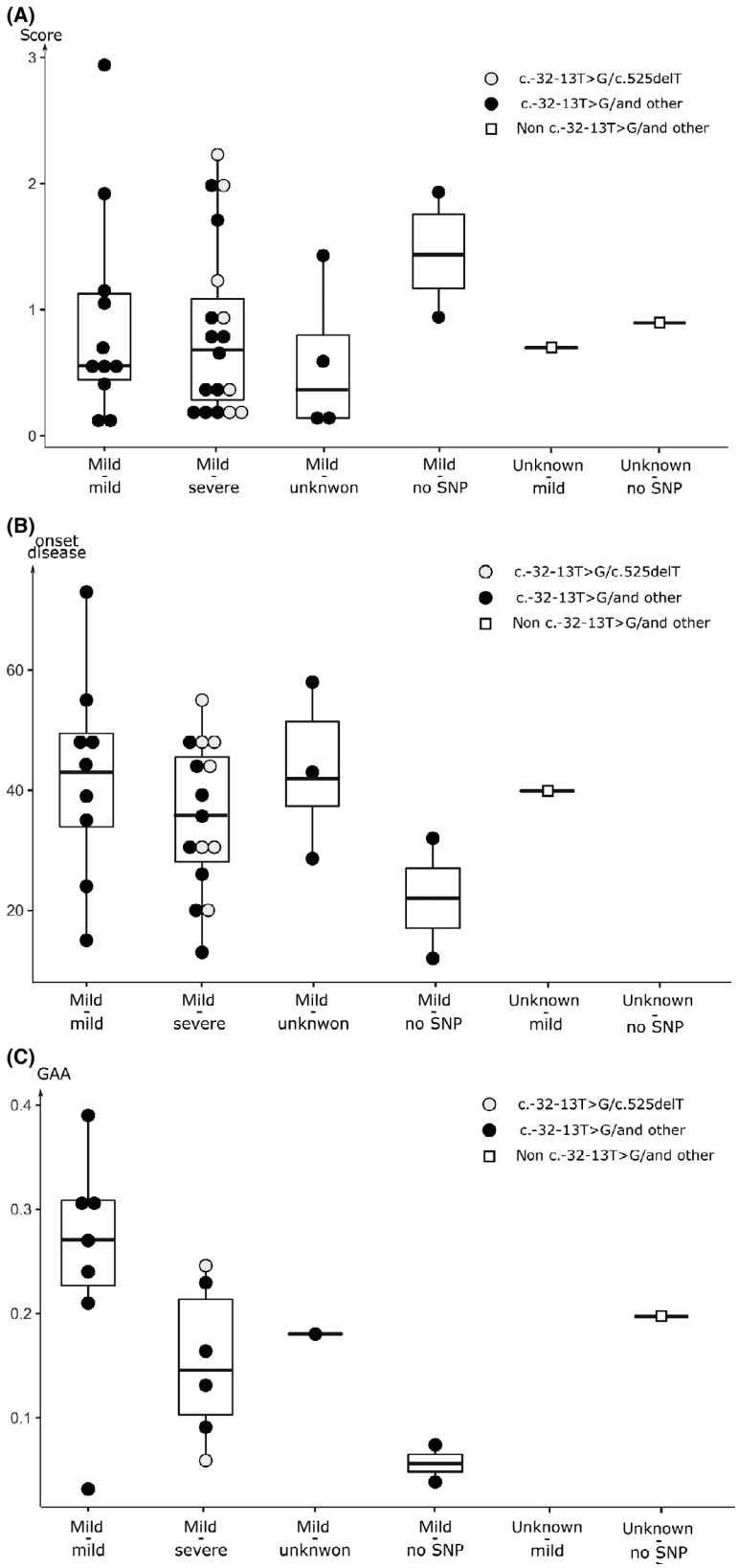

pathology [30]. But even early therapy does not predict a good clinical outcome in all patients [10,32,33]. However, the underlying reason why the efficiency of therapy is restricted is not fully understood. Here, we translate this morpho-score to the muscle analysis in LOPD. Although, muscle pathology in LOPD patients has been reported earlier, our cohort encompasses the highest number of tissue specimens investigated in detail so far [17,22,23,29]. In our study, LOPD muscle biopsy samples show a high variability in muscle morphology. Interestingly, 75% of the specimens have minor muscle damage with a glycogen accumulation of <10% and a morpho-score below grade 1. On average, the morpho-score is much lower in LOPD compared to IOPD, which shows muscle pathology before the start of ERT with scores up to 4, as expected by a higher residual GAA enzyme activity in LOPD [17,21]. Muscle biopsies from LOPD patients can show a subtle pathology and sometimes are graded as unspecific on PAS stained cryosections [34]. In the present study, although in four patients the morpho-score was low, glycogen containing vacuoles were present in all of them on PAS-stained resin sections.

Treatment with recombinant GAA leads to decreased intra-lysosomal glycogen accumulation [35]. In our study even in muscle biopsy specimens with a low morpho-score, extra-lysosomal glycogen was detectable, but without major disruption of the sarcomeric structure. Whereas high morpho-scores were associated with large extra-lysosomal glycogen deposits and severe sarcomeric disorganization. The morpho-score and glycogen accumulation correlated with increased endomysial fibrosis, informing about severe stages of muscle damage with increased connective tissue replacement. Recently, analyses of glycogen clearance in LOPD muscle samples showed that free extra-lysosomal cytoplasmic glycogen persisted in post-treatment biopsy specimens, suggesting that ERT treatment may have been introduced too late, but neither fibrosis nor sarcomeric disorganisation was described [22].

The age and gender distribution of our cohort reveals a median age of 41 years, 55% of patients were male patients and a diagnostic delay of 5 years, consistent with other reports [9,17,29]. Correlating muscle pathology with disease duration shows that patients with longer disease duration do not have more severe muscle tissue damage. These data underscore the clinical heterogeneity and indicate that additional factors may contribute to disease progression and severity. Interestingly, serum CK levels were lower in older patients, possibly related to disease associated muscle atrophy.

In mechanically strained striated MFs, autophagy is an important process for normal cell function, and dysfunction of autophagy plays a major role in disease progression in lysosomal myopathies [24,36]. In Pompe disease, autophagy is impaired with autophagic buildup of various degree in both IOPD and LOPD showing large vacuoles and increase of autophagy markers, LC3 and p62, which might accelerate the muscle damage [37–39]. Large vacuoles and large glycogen deposits remain unchanged on ERT treatment, whereas a reduction in glycogen is associated with a reduction in vacuolated fibres [29].

Therapeutic benefits by modifying autophagy in Pompe disease have been demonstrated in several animal models [40–43]. In our study, buildup of autophagy showed a significant positive correlation with the morpho-score and glycogen accumulation, highlighting the role of autophagy in severe stages of LOPD muscle pathology. The autophagic markers, LC3 and p62 correlated with the lysosomal enzyme acid phosphatase and were increased in muscle biopsies with more severe pathology. Tension induced accumulation of proteins in skeletal MFs are degraded by chaperone-assisted selective autophagy in which the co-chaperone BAG3 plays an important role [44]. Interestingly in our study, small BAG3 positive inclusions were present mostly in the core of preserved MFs suggesting that BAG3 is involved in early events and not at late stage pathology. BAG3 has been found to be located inside autophagosomes and triggers the autophagy of ubiquitinated clients [45], which is in line with large autophagosomes found at ultrastructural analysis in MFs in our study. These observations also fit well with autophagic buildup observed in the core of the MFs in GAA mice [37]. The autophagic buildup seems to disrupt sarcomere structure and leads to loss of muscle force rather than buildup of glycogen filled lysosomes [46]. Further studies are necessary to investigate the role of BAG3 in the autophagic process in Pompe disease in more detail.

Countries with new-born screening for Pompe disease are increasing and in addition, to the early genetic diagnosis of IOPD, a large number of mutations in *GAA* associated with LOPD are being detected and are of an

uncertain clinical outcome [47,48]. Over 500 different pathogenic *GAA* mutations are known and affected individuals show high phenotypic variability despite sharing the same *GAA* mutations, even within a family [3,7,32]. Until now, only a few factors such as angiotensin enzyme polymorphisms have been reported to modify the individual Pompe disease phenotype [5]. The c.-32-13T>G mutation is the most common *GAA* mutation in Europe. In individuals with compound heterozygous mutations, disease manifestation may be highly variable regarding both age of onset and initial symptoms [4,6,7,16,49,50]. In our cohort of 37 German LOPD patients, 95% are compound heterozygous with the c.-32-13T>G mutation on one allele, and show symptom onset at a mean age of 39 years (12–73 year), consistent with published data [4]. The high variability of mutations affecting the second allele, with the most common combination being with c.525delT in 19% in our patients along with several other less common mutations, makes correlative analysis difficult. Our analysis does not show differences in the morpho-score or disease onset between different allele combinations. Therefore, we ranked the phenotype of the mutations according to the Pompe mutation database. We studied different allele combinations to elucidate whether patients with different combinations had distinct clinical features, ages of onset or muscle pathology [2]. The majority of the LOPD patients had a combination of a mild with a severe *GAA* (49%). However, clinical findings and muscle morphology do not relate to the genetic findings in the investigated patient group. Therefore, a genotype–phenotype correlation cannot be defined.

Conclusion

The detailed analysis of muscle morphology in a large cohort of patients with LOPD reflects high variability of muscle tissue damage. This variability is accompanied by moderate glycogen accumulation and a low morpho-score in most patients. High morpho-scores are associated with increased fibrosis and autophagy. This highlights the role of autophagy in severe stages of muscle tissue damage. Comparing muscle morphology and genetic findings reveals no meaningful genotype–phenotype correlations. This emphasises the putative relevance of yet unknown genetic modifiers independent of the *GAA* mutational spectrum. Transcriptomics, proteomics and metabolomics studies need to be performed to address these open questions.

Ethical statement

This work was in accordance with the ethical standards of the responsible committee on human experimentation (ethical committee of the University of Giessen; AZ07/09) and with the Helsinki Declaration (1964, amended most recently in 2008) of the World Medical Association and written informed consent was obtained from the patients.

Acknowledgements

We thank the patients contributing to the study. We thank Angela Roth, Hannah Schlierbach and Kerstin Leib for her excellent technical assistance and the Institute of Neuropathology WWU Muenster, Germany for contributed muscle biopsy samples.

Author contributions

AS designed the study, analysed data and wrote the manuscript. MK and LV performed morphometric analyses of muscle biopsies and analysed data. CK, KC, UP, PY, MB, IS, MB. CM, SV, JW, MD, AZ, WS, BS contributed muscle biopsy samples, clinical data and reviewed the manuscript. DN and AH assisted with the interpretation of genetic data and IWM with statistical analysis. All authors read and approved the final manuscript.

Funding

For this analysis unrestricted research funding was given to AS by Sanofi-Aventis Deutschland GmbH.

Conflict of interest

The authors have no conflicts of interest in respect of the manuscript contents. The Editors of Neuropathology and Applied Neurobiology are committed to peer-review integrity and upholding the highest standards of review. As such, this article was peer-reviewed by independent, anonymous expert referees and the authors (including WS) had no role in either the editorial decision or the handling of the paper.

References

1 Hoefsloot LH, Hoogeveen-Westerveld M, Reuser AJ, Oostra BA. Characterization of the human lysosomal alpha-glucosidase gene. *Biochem J* 1990; **272**: 493–7

2 Kroos M, Hoogeveen-Westerveld M, Michelakakis H, Pomponio R, Van der Ploeg A, Halley D, et al. Update of the pompe disease mutation database with 60 novel GAA sequence variants and additional studies on the functional effect of 34 previously reported variants. *Hum Mut* 2012; **33**: 1161–5

3 Kroos M, Hoogeveen-Westerveld M, van der Ploeg A, Reuser AJ. The genotype-phenotype correlation in Pompe disease. *Am J Med Genet C Semin Med Genet* 2012; **160**: 59–68

4 Kroos MA, Pomponio RJ, Hagemans ML, Keulemans JL, Phipps M, DeRiso M, et al. Broad spectrum of Pompe disease in patients with the same c.-32-13T->G haplotype. *Neurology* 2007; **68**: 110–5

5 De Filippi P, Saeidi K, Ravaglia S, Dardis A, Angelini C, Mongini T, et al. Genotype-phenotype correlation in Pompe disease, a step forward. *Orphanet J Rare Dis* 2014; **9**: 102

6 Montagnese F, Barca E, Musumeci O, Mondello S, Migliorato A, Ciranni A, et al. Clinical and molecular aspects of 30 patients with late-onset Pompe disease (LOPD): unusual features and response to treatment. *J Neurol* 2015; **262**: 968–78

7 Wens SC, van Gelder CM, Kruijshaar ME, de Vries JM, van der Beek NA, Reuser AJ, et al. Phenotypical variation within 22 families with Pompe disease. *Orphanet J Rare Dis* 2013; **8**: 182

8 Sampaolo S, Esposito T, Farina O, Formicola D, Diodato D, Gianfrancesco F, et al. Distinct disease phenotypes linked to different combinations of GAA mutations in a large late-onset GSDII sibship. *Orphanet J Rare Dis* 2013; **8**: 159

9 Löscher WN, Huemer M, Stulnig TM, Simschitz P, Iglseder S, Eggers C, et al. Pompe disease in Austria: clinical, genetic and epidemiological aspects. *J Neurol* 2018; **265**: 159–64

10 Hahn A, Praetorius S, Karabul N, Diessel J, Schmidt D, Motz R, et al. Outcome of patients with classical infantile pompe disease receiving enzyme replacement therapy in Germany. *JIMD Rep* 2015; **20**: 65–75

11 Montalvo AL, Bembi B, Donnarumma M, Filocamo M, Parenti G, Rossi M, et al. Mutation profile of the GAA gene in 40 Italian patients with late onset glycogen storage disease type II. *Hum Mut* 2006; **27**: 999–1006

12 Hirschhorn R, Reuser AJJ. Glykogen storage disease type II: acid alpha-glucosidase (acid maltase) defiency. In *The Metabolic and Molecular Bases of Inherited Disease*. Chapter 135. Eds D Valle, O Simell. New York: McGraw-Hill, 2001; 3389–420

13 Kishnani PS, Steiner RD, Bali D, Berger K, Byrne BJ, Case LE, et al. Pompe disease diagnosis and management guideline. *Genet Med* 2006; **8**: 267–88

14 van den Hout HM, Hop W, van Diggelen OP, Smeitink JA, Smit GP, Poll-The BT, et al. The natural course of infantile Pompe's disease: 20 original cases compared with 133 cases from the literature. *Pediatrics* 2003; **112**: 332–40

15 Winkel LP, Hagemans ML, van Doorn PA, Loonen MC, Hop WJ, Reuser AJ, et al. The natural course of non-classic Pompe's disease; a review of 225 published cases. *J Neurol* 2005; **252**: 875–84

16 Herzog A, Hartung R, Reuser AJ, Hermanns P, Runz H, Karabul N, et al. A cross-sectional single-centre study on the spectrum of Pompe disease, German patients: molecular analysis of the GAA gene, manifestation and genotype-phenotype correlations. *Orphanet J Rare* 2012; **7**: 35

17 Schoser BG, Müller-Höcker J, Horvath R, Gempel K, Pongratz D, Lochmüller H, et al. Adult-onset glycogen storage disease type 2: clinico-pathological phenotype revisited. *Neuropathol Appl Neurobiol* 2007; **33**: 544–59

18 Joshi PR, Glaser D, Schmidt S, Vorgerd M, Winterholler M, Eger K, et al. Molecular diagnosis of German patients with late-onset glycogen storage disease type II. *J Inherit Metabol Dis* 2008; **31** (Suppl. 2): S261–5

19 Gungor D, de Vries JM, Hop WC, Reuser AJ, van Doorn PA, van der Ploeg AT, et al. Survival and associated factors in 268 adults with Pompe disease prior to treatment with enzyme replacement therapy. *Orphanet J Rare* 2011; **6**: 34

20 Toscano A, Schoser B. Enzyme replacement therapy in late-onset Pompe disease: a systematic literature review. *J Neurol* 2013; **260**: 951–9

21 Schänzer A, Kaiser AK, Mühlfeld C, Kulessa M, Paulus W, von Pein H, et al. Quantification of muscle pathology in infantile Pompe disease. *Neuromusc Dis* 2017; **27**: 141–52

22 van der Ploeg A, Carlier PG, Carlier RY, Kissel JT, Schoser B, Wenninger S, et al. Prospective exploratory muscle biopsy, imaging, and functional assessment in patients with late-onset Pompe disease treated with alglucosidase alfa: the EMBASSY Study. *Mol Genet Metabol* 2016; **119**: 115–23

23 Müller-Felber W, Horvath R, Gempel K, Podskarbi T, Shin Y, Pongratz D, et al. Late onset Pompe disease: clinical and neurophysiological spectrum of 38 patients including long-term follow-up in 18 patients. *Neuromusc Dis* 2007; **17**: 698–706

24 Malicdan MC, Nishino I. Autophagy in lysosomal myopathies. *Brain Pathol* 2012; **22**: 82–8

25 Nascimbeni AC, Fanin M, Tasca E, Angelini C, Sandri M. Impaired autophagy affects acid alpha-glucosidase processing and enzyme replacement therapy efficacy in late-onset glycogen storage disease type II. *Neuropathol Appl Neurobiol* 2015; **41**: 672–5

26 Raben N, Wong A, Ralston E, Myerowitz R. Autophagy and mitochondria in Pompe disease: nothing is

so new as what has long been forgotten. *Am J Med Genet* 2012; **160**: 13–21
27 Chien YH, Lee NC, Huang PH, Lee WT, Thurberg BL, Hwu WL. Early pathologic changes and responses to treatment in patients with later-onset Pompe disease. *Pediatr Neurol* 2012; **46**: 168–71
28 Feeney EJ, Austin S, Chien YH, Mandel H, Schoser B, Prater S, et al. The value of muscle biopsies in Pompe disease: identifying lipofuscin inclusions in juvenile- and adult-onset patients. *Acta Neuropathol Comm* 2014; **2**: 2
29 Ripolone M, Violano R, Ronchi D, Mondello S, Nascimbeni A, Colombo I, et al. Effects of short-to-long term enzyme replacement therapy (ERT) on skeletal muscle tissue in late onset Pompe disease (LOPD). *Neuropathol Appl Neurobiol* 2018; **44**: 449–62
30 Thurberg BL, Lynch Maloney C, Vaccaro C, Afonso K, Tsai AC, Bossen E, et al. Characterization of pre- and post-treatment pathology after enzyme replacement therapy for Pompe disease. *Lab Invest* 2006; **86**: 1208–20
31 Dubowitz V, Sewry C, Oldfords A. *Muscle Biopsy: A Practical Approach*. London: Saunders Elsevier, 2013
32 Schänzer A, Giese K, Viergutz L, Hahn A. Letter to the editors: concerning 'divergent clinical outcomes of alpha-glucosidase enzyme replacement therapy in two siblings with infantile-onset Pompe disease treated in the symptomatic or pre-symptomatic state' by Takashi et al. and Letter to the Editors by Ortolano et al. *Mol Genet Metabol Rep* 2017; **12**: 33–4
33 Schänzer A, Görlach J, Claudi K, Hahn A. Severe distal muscle involvement and mild sensory neuropathy in a boy with infantile onset Pompe disease treated with enzyme replacement therapy for 6 years. *Neuromusc Disord* 2019; **29**: 477–82
34 Golsari A, Nasimzadah A, Thomalla G, Keller S, Gerloff C, Magnus T. Prevalence of adult Pompe disease in patients with proximal myopathic syndrome and undiagnosed muscle biopsy. *Neuromusc Dis* 2018; **28**: 257–61
35 Reuser AJ, Van Den Hout H, Bijvoet AG, Kroos MA, Verbeet MP, Van Der Ploeg AT. Enzyme therapy for Pompe disease: from science to industrial enterprise. *Eur J Pediatr* 2002; **161** (Suppl. 1): S106–11
36 Neel BA, Lin Y, Pessin JE. Skeletal muscle autophagy: a new metabolic regulator. *Trends Endocrinol Metabol* 2013; **24**: 635–43
37 Raben N, Hill V, Shea L, Takikita S, Baum R, Mizushima N, et al. Suppression of autophagy in skeletal muscle uncovers the accumulation of ubiquitinated proteins and their potential role in muscle damage in Pompe disease. *Hum Mol Genet* 2008; **17**: 3897–908
38 Nascimbeni AC, Fanin M, Masiero E, Angelini C, Sandri M. Impaired autophagy contributes to muscle atrophy in glycogen storage disease type II patients. *Autophagy* 2012; **8**: 1697–700
39 Lim JA, Li L, Raben N. Pompe disease: from pathophysiology to therapy and back again. *Front Aging Neurosci* 2014; **6**: 177
40 Lim JA, Sun B, Puertollano R, Raben N. Therapeutic benefit of autophagy modulation in Pompe disease. *Mol Ther* 2018; **26**: 1783–96
41 Lim JA, Li L, Shirihai OS, Trudeau KM, Puertollano R, Raben N. Modulation of mTOR signaling as a strategy for the treatment of Pompe disease. *EMBO Mol Med* 2017; **9**: 353–70
42 Raben N, Schreiner C, Baum R, Takikita S, Xu S, Xie T, et al. Suppression of autophagy permits successful enzyme replacement therapy in a lysosomal storage disorder–murine Pompe disease. *Autophagy* 2010; **6**: 1078–89
43 Lim J, Meena N, Raben N. Pros and cons of different ways to address dysfunctional autophagy in Pompe disease. *Ann Trans Med* 2019; **7**: 279
44 Ulbricht A, Gehlert S, Leciejewski B, Schiffer T, Bloch W, Höhfeld J. Induction and adaptation of chaperone-assisted selective autophagy CASA in response to resistance exercise in human skeletal muscle. *Autophagy* 2015; **11**: 538–46
45 Klimek C, Kathage B, Wordehoff J, Höhfeld J. BAG3-mediated proteostasis at a glance. *J Cell Sci* 2017; **130**: 2781–8
46 Xu S, Galperin M, Melvin G, Horowits R, Raben N, Plotz P, et al. Impaired organization and function of myofilaments in single muscle fibers from a mouse model of Pompe disease. *J Appl Physiol* 2010; **108**: 1383–8
47 Chien YH, Lee NC, Thurberg BL, Chiang SC, Zhang XK, Keutzer J, et al. Pompe disease in infants: improving the prognosis by newborn screening and early treatment. *Pediatrics* 2009; **124**: e1116–25
48 Chien YH, Lee NC, Huang HJ, Thurberg BL, Tsai FJ, Hwu WL. Later-onset Pompe disease: early detection and early treatment initiation enabled by newborn screening. *J Pediatr* 2011; **158**: 1023–7.e1
49 Huie ML, Chen AS, Tsujino S, Shanske S, DiMauro S, Engel AG, et al. Aberrant splicing in adult onset glycogen storage disease type II (GSDII): molecular identification of an IVS1 (-13T–>G) mutation in a majority of patients and a novel IVS10 (+1GT–>CT) mutation. *Hum Mol Genet* 1994; **3**: 2231–6
50 Johnson K, Topf A, Bertoli M, Phillips L, Claeys KG, Stojanovic VR, et al. Identification of GAA variants through whole exome sequencing targeted to a cohort of 606 patients with unexplained limb-girdle muscle weakness. *Orphanet J Rare* 2017; **12**: 173
51 R Core Team. *R: A language and environment for statistical computing*. Vienna, Austria: R Foundation for Statistical Computing, 2018. Available at https://www.R-project.org/

Supporting information

Additional Supporting Information may be found in the online version of this article at the publisher's web-site:

Figure S1. For estimating the morpho-score Periodic acid-Schiff (PAS) stained resin sections were graded from 0 to 5: grade 0 = normal, grade 1 = small PAS + vacuoles, grade 2 = medium PAS + vacuoles, grade 3 = larger PAS + vacuoles with myofibrillar disruption, grade 4 = larger PAS + vacuoles and large empty vacuoles (LEV) with myofibrillar disruption, grade 5 = LEV with myofibrillar disruption (**A**). Muscle sections show muscle fibres with different grading close to each other (**B**,**C**). (**A**–**C**: PAS stained resin sections, magnification × 400).

Figure S2. Staining intensity of acid phosphatase and expression of autophagy markers microtubule-associated protein 1A/1B-light chain 3 and p62 in patients with different morpho-scores. Muscle biopsies with a higher morpho-scores shows increased expression compared to muscle biopsies with a lower score (**A**). Correlation matrix of score, Periodic acid-Schiff (PAS), large empty vacuoles (LEV), autophagic vacuoles (AV) and fibrosis obtained from the muscle biopsies. Upper triangular part of the matrix shows the spearman correlation coefficients (Spearman's rho with significance levels associated to a symbol (*P*-values: ***<0.001, **<0.01, *<0.05). The distribution of each variable is shown on the diagonal (blue). Lower triangular part of the matrix shows the bivariate scatterplots (blue) with a fitted line (black) and the confidence interval of the line (grey) The morpho-score shows a significant positive correlation with p62 and acid phosphatase compatible with increased autophagy and lysosomal activity during muscle pathology progression (**B**).

Figure S3. With double immunofluorescent staining against Z-band proteins desmin (green) and Bcl2-associated athanogene 3 (BAG3) (red) small BAG3 positive inclusions in the core of muscle fibres (MFs) can be detected mostly in well-preserved MFs and are increased in muscle biopsies with high expression of microtubule-associated protein 1A/1B-light chain 3 and p62. In vacuolated fibres sarcomeric remnants show co-expression of desmin and BAG3 (yellow) and no larger BAG3 positive inclusions.

Figure S4. Ultrastructural analysis of muscle biopsies in which immunofluorescence staining against Bcl2-associated athanogene 3 (BAG3) was performed: large autophagosomes are located mainly in the muscle fibre (MF) core. Only focal loss of Z-bands is noted at higher magnification accompanied by swollen microtubules, small vacuoles and intra- and extra-lysosomal glycogen (P53). In single MFs with more severe sarcomere disarray or large areas of glycogen accumulation no increased large autophagosomes are present (P33, P41). Muscle fibres with upregulation of microtubule-associated protein 1A/1B-light chain 3 expression show increased numbers of large autophagosomes (P30).

Figure S5. Analyses of alpha 1,4-glucosidase (*GAA*) gene mutations compared to muscle morphology and clinical data: Boxplots of the individual morpho-score to *GAA* gene mutation combination. The combinations for each subject are shown as points, and the box and whisker plots show the quartiles and medians (solid horizontal line within the boxes). The whiskers add 1.5 times the interquartile range (IQR) to the 75th percentile or subtract 1.5 times the IQR from the 25th percentile. The global differences between the individual scores to mutation combination did not met statistical significance ($P > 0.1$). According to the Pompe Disease Mutation Database mutations were ranked as mild (potential less severe mutation); severe, (very severe mutation); unknown, (unknown mutation) and no single nucleotide polymorphism (SNP) (AV, autophagic vacuoles; LEV, large empty vacuoles). No significant differences are detectable analysing the vacuoles (AV or LEV) with respect to the *GAA* genotype.

Table S1. Clinical data and genetic background of the patients with late onset Pome disease.

Table S2. Morphological data of the patients with late onset Pome disease.

Table S3. Analysis of autophagy markers in patients with late onset Pome disease.

Received 21 June 2019
Accepted after revision 7 August 2019
Published online Article Accepted on 23 September 2019